Slip and Slide Detection and Adaptive Information Sharing Algorithms for High-Speed Train Navigation Systems

Kwanghoon Kim, Seung-Hyun Kong, *Member, IEEE*, and Sang-Yun Jeon

***Abstract*—The position and velocity information of high-speed trains (HSTs) are essential to passenger safety, operational efficiency, and maintenance, for which an accurate navigation system is required. In this paper, we propose a two-stage federated Kalman filter (TS-FKF) for an HST navigation system that uses multi-sensors, such as tachometer, inertial navigation system, differential GPS, and RFID, with a feedback scheme. However, the FKF with a feedback scheme often shows severe performance degradation in the presence of undetected large sensor errors. Tachometers often have large slip or slide errors during the train's acceleration, deceleration, and moving along a curved railway, and there are significant performance differences between different sensors. To make the proposed system robust to these errors, we propose a slip and slide detection algorithm for the tachometer and an adaptive information-sharing algorithm to deal with a large tachometer error and performance difference between sensors. We provide theoretical analysis and simulation results to demonstrate the performance of the proposed navigation system with the proposed algorithms.**

***Index Terms*—Train navigation system, positioning, slip and slide detection, sensor fusion, federated Kalman filter, information sharing.**

I. Introduction

HIGH-SPEED trains (HSTs) are becoming a popular transportation system in Europe, China, and Korea, and there have been a number of research and developments (R&D) for the HST [1]–[3]. In Korea, Korean Railroad Research Institute and Hyundai Rotem Inc. are leading the development of a new HST called HEMU-430X [3] whose target maximum speed is 400 Km/h. To put HEMU-430X to practical use in near future, there have been many R&D efforts to enhance the performance of the HST in diverse aspects. Among them, an HST navigation system with higher accuracy and reliability is the one of the most integral parts to improve passenger safety, operational efficiency, and maintenance that are not supported by the conventional train navigation system based on the track circuits. As there are various positioning sensors applicable to HST navigation systems, it is possible to develop a very accurate navigation system that provides less than a meter-level accuracy error in average for the HSTs such as HEMU-430X. However, the development of such an HST navigation system requires good solutions for the following three problems in practice.

First, we need to use accurate, reliable, and inexpensive sensors and need to have a multi-sensor fusion algorithm that provides good performance in various train environments. For example, differential global positioning system (DGPS) can provide meter-level accuracy in the open-sky environments. However, DGPS fails to produce position fixes in tunnels and often shows severe accuracy degradation in urban canyon, for which a navigation system needs to utilize other reliable sensors such as inertial navigation system (INS) and tachometers to have robust positioning performance [2], [4]. In addition, the HST may require more reliable and accurate positioning performance than DGPS, INS, and tachometers. For example, HEMU-430X is planning to use an RFID based positioning scheme that acquires precise position information from RFID tags at precisely known locations [3]. In general, a multi-sensor based navigation system may not use a feedback scheme in the filter in order to prevent the system from malfunctioning due to a particular sensor failure or large sensor errors, where some system performance degradation is inevitable as the system utilizes the sensor output.

Second, an HST navigation system based on multi-sensors may need a fault-detection scheme. Sensors such as INS, RFID, and DGPS have a very small probability of sensor failure in normal conditions. DGPS may not provide a position fix in tunnels and shadowing area, which is only an outage of service for a limited time duration [5]. And, in general, we can expect the GPS outage using a map and train's motion so that the GPS outage should be treated differently from a mere sensor failure. In case of tachometers, however, it suffers from potentially large slip and slide errors that occur during the train's acceleration, deceleration, and moving along a curved railway. In general, wheel slip occurs when the wheel is rotating faster than a nominal wheel while wheel slide occurs when the wheel is rotating slower than a nominal wheel [6]. Depending on the

Manuscript received October 9, 2014; revised February 11, 2015, March 31, 2015, and May 3, 2015; accepted May 22, 2015. Date of publication June 15, 2015; date of current version November 23, 2015. This work was supported by a grant from the Development of GNSS-based Transportation Infrastructure Technology funded by the Ministry of Land, Transport and Maritime Affairs of the Korean government. The Associate Editor for this paper was D. Chen. *(Corresponding author: Seung-Hyun Kong.)*

K. Kim is with LIG Nex1, Yongin 446-798, Korea (e-mail: khkim73@kaist.ac.kr).

S.-H. Kong and S.-Y Jeon are with the CCS Graduate School for Green Transportation, Korea Advanced Institute of Science and Technology, Daejeon 305-701, Korea (e-mail: skong@kaist.ac.kr; jeonsyun@kaist.ac.kr).

Color versions of one or more of the figures in this paper are available online at http://ieeexplore.ieee.org.

Digital Object Identifier 10.1109/TITS.2015.2437899

TABLE I
PERFORMANCE CHARACTERISTICS OF THE SENSORS

	Advantage	Disadvantage
DGPS	High accuracy and reliability in most outdoor environments	Outage in tunnels and performance degradation in urban canyons
INS	High short term accuracy and reliability	Polynomial accuracy degradation with respect to time
Tacho -meter	High short term accuracy and reliability	Polynomial accuracy degradation in the presence of slip and slide
RFID	High momentary accuracy and reliability at intermittent locations	Overall performance depends on deployment density

rail condition and the train's motion, the tachometer errors can occur frequently and continuously degrades the performance of the navigation system. In the literature, there have been a number of studies on the slip and slide detection (SSD). In [7], [8], the slip detection is studied for autonomous mobile robots and vehicles in dynamic motions. In [9], tachometer readings from four wheels, at the front-left, front-right, rear-left, and rear-right, are used to estimate a slip or a slide, which may not be efficient for trains with no propeller shaft and brake shaft. In [10], tachometer readings are compared with thresholds to detect the wheel slip and slide, which may not be adequate for the HST that requires a precise positioning. As a good reference, velocity estimation from a GPS receiver is used to compare with tachometer readings and to detect the wheel slip and slide [6]. And in [11], the authors use a Kalman filter (KF) to estimate the velocity and acceleration of the train and propose a slip and slide detection (SSD) technique to compare tachometer readings with the estimated states. In a viewpoint, the previous studies on the SSD are based on a mere comparison to a reference value measured by a single sensor such as GPS or on the mutual comparison of tachometer readings.

Third, the HST navigation system should be carefully designed to deal with the performance difference between difference sensors as summarized in Table I. In [12], [13], multi-sensor outputs are combined using an FKF, where each sensor is assumed to have the same error variance. However, this assumption may not be valid in practice and determining the information sharing factor (ISF) affects significant effect for the HST navigation system. Liu proposes an algorithm to compute ISF by comparing the inverse of the norm of the error covariance of each local filter [14], which considers only the error covariance. In [15], Qiuping considers GPS constellation in the determination of the ISF for a vehicular application, which is, however, not applicable to other applications that do not use GPS. Zhang proposes an algorithm to compute the ISF based on the generalized eigenvalue decomposition of the error covariance of each local filter [16], and Zhi proposes an algorithm to compute the ISF using the eigenvalue of the error covariance and the singular value of the observability matrix [17]. In general, the algorithms in [16], [17] are computationally too expensive to applications requiring fast real-time computation.

Therefore, to improve robustness to the sensor failure and to maintain high performance with various sensors of different performance in real-time, it is necessary for the KF based HST navigation systems to be equipped with an appropriate low computational IS algorithm and SSD algorithm. In this paper, we consider the above three problems in the development of an accurate and reliable HST navigation system for HEMU-430X. Since federated Kalman filter (FKF) requires low computational cost to process multi-sensor outputs [13], and a feedback scheme with IS and SSD algorithms can be easily implemented in two-stage FKF (TS-FKF), we propose an HST navigation system based on TS-FKF with a feedback scheme (for IS and SSD) in Section II. The proposed navigation system employs multi-sensors such as tachometer, INS, DGPS, and RFID. We provide theoretical expressions for each local filter associated with each sensor and for two master filters of the TS-FKF. The output of the proposed navigation system can be used to detect the slip and slide errors, which provides an improved performance comparing to other SSD techniques using reference from a single sensor. In Section III, we propose an adaptive information sharing (IS) algorithm to weight and distribute the error covariance. In Section IV, we propose two SSD algorithms based on the position and velocity. Since the proposed TS-FKF utilizes a feedback scheme, it is required to automatically evaluate the performance of each local filter and to appropriately combine the estimated information from local filters. The IS algorithm is to distribute the error covariance to local filters based on each local filter performance, and the SSD algorithm is to detect and to eliminate large tachometer errors such as the slip and slide errors. In Section V, we perform various simulations to compare the performance of the IS and SSD algorithms in order to determine the best IS and SSD algorithms in performance and cost for the proposed navigation system. And in Section VI, we draw a conclusion of the paper.

II. HIGH-SPEED TRAIN NAVIGATION SYSTEM BASED ON TWO-STAGE FEDERATED KALMAN FILTER

A. Fault-Tolerant Train Navigation System

The proposed HST navigation system has a TS-FKF structure, as shown in Fig. 1, with an SSD algorithm to improve tachometer error detection and with an IS algorithm to distribute the error covariance. The IS and SSD algorithms are described in detail in Sections III and IV, respectively. In this section, we provide a brief introduction to the TS-FKF, and the details for local filters associated with multi-sensors can be found in [3], [18]. As shown in Fig. 1, the output of the INS is used as a primary sensor output and is fed into each local filter. There are four different sensors; tachometer and DGPS provide velocity measurements, and DGPS and RFID provide position measurements. Note that DGPS can provide velocity and position measurements that can be assumed uncorrelated, since the measurements are from Doppler observation and code phase observation separately in the GPS receiver, respectively. The difference between the output of each sensor and INS is used as the measurement to each local filter. There are four local filters associated with the four sensors, and there are two FKF master filters. The first FKF master filter provides a reference to the SSD algorithm, and the second FKF master filter is

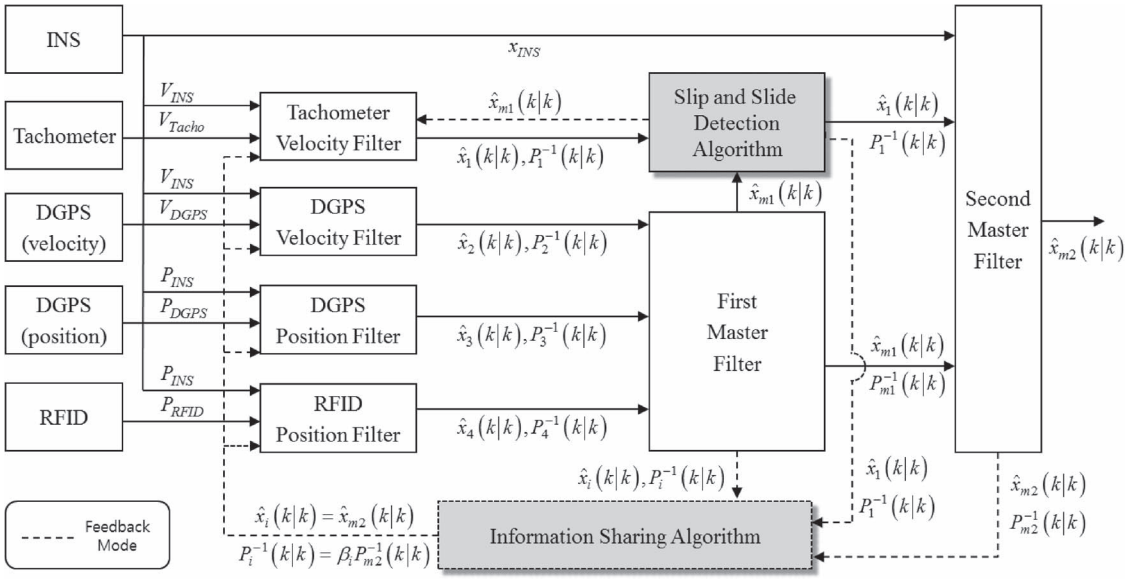

Fig. 1. Structure of the proposed train navigation system.

associated with the IS algorithm. In Section II-B and C, we provide algebraic expressions for the details of local filters and master filters, respectively.

B. Local Filter Design

1) System Equation for INS: The INS error model is readily available from the INS pure navigation equations using the perturbation method [18] and is used to derive the INS system equation as

$$\delta\dot{x}(t) = F_{INS}(t)\delta x(t) + G(t)w(t), \tag{1}$$

where F_{INS} is the system matrix, $w(t)$ is a white Gaussian noise with zero mean and covariance $Q(t)$, and $\delta x(t)$ represents the error state of the system. Exploiting [3], the error state is defined as

$$\delta x(t) = \begin{bmatrix}\delta P & \delta V^n & \delta Q_b^n & \nabla & \eta\end{bmatrix}^T \tag{2a}$$

$$w(t) = \begin{bmatrix}w_a & w_g\end{bmatrix}^T, \tag{2b}$$

where $\delta P = [\delta L\ \delta l\ \delta h]$, $\delta V^n = [\delta V_N\ \delta V_E\ \delta V_D]$, $\delta Q_b^n = [\delta q_0\ \delta q_1\ \delta q_2\ \delta q_3]$, $\nabla = [\nabla_X\ \nabla_Y\ \nabla_Z]$, and $\eta = [\eta_X\ \eta_Y\ \eta_Z]$ define the position error vector in the ECEF coordinate system (latitude, longitude, and height), the velocity error vector defined in the navigation frame, the quaternion error vector, the accelerometer bias error vector in the body frame, and gyroscope bias error vector in the body frame, respectively. The accelerometer errors include a white Gaussian noise vector $w_a = [\ w_{aX}\ w_{aY}\ w_{aZ}\ ]$ and bias error vector ∇ that is random but assumed constant during system operation. Similarly, gyroscope error vector is composed of a white Gaussian noise vector $w_g = [\ w_{gX}\ w_{gY}\ w_{gZ}\ ]$ and a bias error vector η that is random but assumed constant during the system operation. The system model F_{INS} and $G(t)$ are readily available from [18] and are described below

$$F_{INS} = \begin{bmatrix} F_{11} & F_{12} & O_{3\times3} & O_{3\times3} & O_{3\times3} \\ F_{21} & F_{22} & F_{23} & F_{24} & O_{3\times3} \\ F_{31} & F_{32} & F_{33} & O_{3\times3} & F_{35} \\ O_{3\times3} & O_{3\times3} & O_{3\times3} & O_{3\times3} & O_{3\times3} \\ O_{3\times3} & O_{3\times3} & O_{3\times3} & O_{3\times3} & O_{3\times3} \end{bmatrix} \tag{3a}$$

$$G(t) = \begin{bmatrix} O_{3\times3} & O_{3\times3} \\ C_b^n & O_{3\times3} \\ O_{3\times3} & -C_b^n \\ O_{3\times3} & O_{3\times3} \\ O_{3\times3} & O_{3\times3} \end{bmatrix}, \tag{3b}$$

where $O_{m\times n}$ and C_b^n are a $m \times n$ zero matrix and a coordinate transformation matrix, respectively and that represents the rotational transformation from the body frame to the navigation frame.

2) Measurement Equations for Sensors; Tachometers, DGPS, and RFID: The proposed navigation system of the HST is based on three sensors as described in Section I, such as tachometers, DGPS, and RFID. The following equations are available from [3] and are used as measurement equations for local filters

$$\begin{aligned} z_{Tacho}(t) &= C_n^b[V_{INS,X}^n] - [V_{Tacho,X}^b] \\ &= H_{Tacho}\delta x(t) + v_{Tacho}(t) \end{aligned} \tag{4a}$$

$$\begin{aligned} z_{DGPS\_V}(t) &= [V_{INS}] - [V_{DGPS}] \\ &= H_{DGPS\_V}\delta x(t) + v_{DGPS\_V}(t) \end{aligned} \tag{4b}$$

$$\begin{aligned} z_{DGPS\_P}(t) &= [P_{INS}] - [P_{DGPS}] \\ &= H_{DGPS\_P}\delta x(t) + v_{DGPS\_P}(t) \end{aligned} \tag{4c}$$

$$\begin{aligned} z_{RFID}(t) &= [P_{INS}] - [P_{RFID}] \\ &= H_{RFID}\delta x(t) + v_{RFID}(t), \end{aligned} \tag{4d}$$

where v_{Tacho}, v_{DGPS_V}, v_{DGPS_P}, and v_{RFID} are velocities measured by the sensors: Tacho, DGPS_V, DGPS_P, and RFID whose error distributions follow zero-mean normal distributions with variances R_{Tacho}, R_{DGPS_V}, R_{DGPS_P}, and R_{RFID}, respectively. In addition, the measurement matrices for velocity information are defined as

$$H_{Tacho} = \begin{bmatrix} O_{1\times3} & C_n^b(1,:) & H_s(1,:) & O_{1\times6} \end{bmatrix} \quad (5a)$$

$$H_{DGPS\_V} = \begin{bmatrix} O_{1\times3} & 1 & 0 & 0 & O_{1\times10} \\ O_{1\times3} & 0 & 1 & 0 & O_{1\times10} \\ O_{1\times3} & 0 & 0 & 1 & O_{1\times10} \end{bmatrix}, \quad (5b)$$

where H_s is defined in Appendix A and the measurement matrices for position information are defined as

$$H_{DGPS\_P} = \begin{bmatrix} 1 & 0 & 0 & O_{1\times13} \\ 0 & 1 & 0 & O_{1\times13} \\ 0 & 0 & 1 & O_{1\times13} \end{bmatrix} \quad (6a)$$

$$H_{RFID} = \begin{bmatrix} 1 & 0 & 0 & O_{1\times13} \\ 0 & 1 & 0 & O_{1\times13} \\ 0 & 0 & 1 & O_{1\times13} \end{bmatrix}. \quad (6b)$$

C. Master Filter Design

While the FKF usually has one master filter [12], [13], the TS-FKF proposed in this paper has two master filters to employ IS and SSD algorithms. The first master filter estimates the state of the system using the measurements of all sensors except the tachometer, and the state estimates are used for the detection of slip and slide errors. The second master filter combines the estimates from the first master filter with the error compensated estimates from the velocity local filter for the tachometer to provide the final state estimates of the proposed navigation system. Therefore, the first master filter is for the SSD algorithm, and the second master filter is for the IS algorithm and produces the final estimates.

1) The First Master Filter Equations: The input to the first master filter includes the estimates from local filters processing DGPS position, DGPS velocity, and RFID position measurements except the velocity estimate from the tachometer. As shown in Fig. 1, the estimation error covariance of the first master filter at a time instant k, i.e., $t = kT_s$ for an update interval T_s, is found as

$$P_{m1}^{-1}(k|k) = \sum_{i=2}^{M} P_i^{-1}(k|k), \quad (7)$$

where $P_i(k|k)$ is the error covariance of the i-th local filter, $P_{m1}(k|k)$ is the error covariance of the first master filter, and M indicates the number of total sensors. In this paper, the 1st local filter is for the tachometer and $M = 4$ as shown in Fig. 1. The estimate of the first master filter is derived as

$$\hat{x}_{m1}(k|k) = P_{m1}(k|k) \left[\sum_{i=2}^{M} P_i^{-1}(k|k)\hat{x}_i(k|k) \right], \quad (8)$$

where $\hat{x}_i(k|k)$ is the estimate of the i-th local filter and $\hat{x}_{m1}(k|k)$ is the estimate of the first master filter, which is then used for the detection of slip and slide errors in the tachometer measurements.

2) The Second Master Filter Equations: The input to the second master filter is the estimates from the first master filter and from the tachometer local filter. The error covariance of the second master filter is expressed as

$$P_{m2}^{-1}(k|k) = \sum_{i=1}^{M} P_i^{-1}(k|k) = P_{m1}^{-1}(k|k) + P_1^{-1}(k|k) \quad (9)$$

where $P_{m2}(k|k)$ is the error covariance of the second master filter, and $m2$ denotes the second master filter. Therefore, the estimate of the second master filter is obtained as

$$\begin{aligned} \hat{x}_{m2}(k|k) &= P_{m2}(k|k) \left[\sum_{i=1}^{M} P_i^{-1}(k|k)\hat{x}_i(k|k) \right] \\ &= P_{m2}(k|k) \left[P_{m1}^{-1}(k|k)\hat{x}_{m1}(k|k) \right. \\ &\qquad \left. + P_1^{-1}(k|k)\hat{x}_1(k|k) \right], \end{aligned} \quad (10)$$

where $\hat{x}_{m2}(k|k)$ is the estimate of the second master filter.

3) Introduction to Conventional Information Sharing: In this subsection, we introduce the principles of the information sharing algorithm proposed by Carlson [12]. With the FKF based on the feedback scheme and information sharing in [11], the initial error covariance bounds are uncorrelated. The estimates of local filters in the FKF with a feedback scheme are mutually independent and there exists no correlation when the initial states of local filters are uncorrelated with each other [12]. The estimate and its error covariance of the master filter are passed to local filters with the following rules in [11].

First rule is that the information sharing factor (ISF) β_i of the i-th local filter should satisfy the following condition:

$$\sum_{i=1}^{M} \beta_i = 1, 0 \le \beta_i \le 1. \quad (11)$$

In the simplest case, it can be that $\beta_i = \beta_{avg} = 1/M$, however, in practice, β_i should be different as the performance of local filters. Second is that the initial values of the estimate and its error covariance sent to the i-th local filter are

$$\hat{x}_i(0) = \hat{x}(0) \quad (12a)$$

$$P_i(0) = \frac{1}{\beta_i} P(0). \quad (12b)$$

Third rule is that the estimate and its error covariance of the master filter passed to the i-th local filter is expressed as

$$\hat{x}_i(k|k) = \hat{x}_m(k|k) \quad (13a)$$

$$P_i(k|k) = \frac{1}{\beta_i} P_m(k|k) \quad (13b)$$

$$Q_i(k) = \frac{1}{\beta_i} Q_m(k), \quad (13c)$$

where Q_i and Q_m are the process noise covariance of the i-th local filter and the master filter, respectively.

III. Information Sharing Algorithm

The ISF β_i is an important parameter to be determined for the reliable performance of the FKF [12], since the error covariance of each local filter is weighted by $1/\beta_i$ ($i = 1, 2, 3, \ldots, M$ in Fig. 1). For example, when the ISF for the i-th local filter is large, a small error covariance is assigned to the i-th local filter from the second master filter in the proposed HST navigation system, in other words, the i-th local filter gains high credit. When all of local filters have the same performance, the master filter assigns the same ISF to all of the local filters.

As we discussed in Section I, recent techniques to determine the ISF are computationally expensive [14], [16], [17], which may be not suitable for real-time applications. Since the residual of a local filter is obtained from the predicted states and measurements, the ISF may be assigned a value simply inversely proportional to the residuals of the local filters. However, in practice, residuals of some local filters are not always available; the DGPS local filter may not be able to produce the state estimate in tunnels and deep urban canyons, and the updates of the RFID local filter is irregular in time when the RFID tags are not placed with the same spacing or the train is not moving at a constant speed.

In this paper, we propose an IS algorithm that has a simple structure to be implemented and requires a low computational cost. In the following, we analyze the conventional and proposed IS algorithms and compare the performance. Let $\eta_{IS}^i(k)$ be an indicator to the performance degradation of the i-th local filter. However, the considered IS algorithms in the following Section III-A and B use slightly different $\eta_{IS}^i(k)$ that is defined explicitly in the each subsection. For given $\eta_{IS}^i(k)$, the ISF is calculated as

$$\beta_i = \frac{\eta_{IS}^i(k)^{-1}}{\sum_{i=1}^{M} \eta_{IS}^i(k)^{-1}}. \tag{14}$$

A. Conventional Information Sharing Algorithm (IS1)

The conventional algorithm to determine ISF assumes that all of the local filters have the same performance. Therefore, β_i is the same to all local filters, and η_{IS}^i is

$$\eta_{IS}^i(k) = 1. \tag{15}$$

The federated Kalman filter suggested by Carlson uses this algorithm for information sharing [12], [13].

B. Proposed Adaptive Information Sharing Algorithm (IS2)

To determine the ISF adaptively in the proposed IS algorithm, i.e., IS2, we employ γ_{IS}^i to represent the difference between the estimate of the second master filter and that of the i-th local filter as

$$\gamma_{IS}^i(k) = \hat{x}_{m2}(k|k) - \hat{x}_i(k|k). \tag{16}$$

Using γ_{IS}^i, we define η_{IS}^i for IS2 as

$$\eta_{IS}^i(k) = \gamma_{IS}^i(k)^T \left[P_{IS}^i(k|k)\right]^{-1} \gamma_{IS}^i(k), \tag{17}$$

where P_{IS}^i is a covariance of γ_{IS}^i.

Since the second master filter generates the best estimates comparing to the local filters because it uses all of sensor information, it is the most reliable to choose the estimate $\hat{x}_{m2}$ of the second master filter as a reference. In (16), γ_{IS}^i represents the distance that the i-th local filter deviates from the reference. However, when we use η_{IS}^i as defined in (17), it should be carefully considered that $\hat{x}_{m2}$ is correlated to $\hat{x}_i$, because $\hat{x}_{m2}$ is obtained from all of the estimates of the local filters. Therefore, the IS2 algorithm deals with this correlation problem when we obtain the covariance P_{IS}^i derived in Lemma B-.1 in Appendix B.

Theorem 1: From Lemma B-.1 and Lemma B-.2 in Appendix B, it is proved that $P_{IS}^i(k) = P_i(k|k) - P_{m2}(k|k)$.

Proof: Since $P_{m2,i}(k|k) = P_{m2}(k|k)$ from Lemma B-.2 and $P_{m2,i}(k|k)$ is equivalent to $P_{i,m2}(k|k)$, (B-.8) is simplified to

$$\begin{aligned} P_{IS}^i(k) &= P_i(k|k) - P_{i,m2}(k|k) - P_{m2,i}(k|k) + P_{m2}(k|k) \\ &= P_i(k|k) - P_{m2}(k|k) - P_{m2}(k|k) + P_{m2}(k|k) \\ &= P_i(k|k) - P_{m2}(k|k). \end{aligned} \tag{18}$$

■

From Theorem 1, η_{IS}^i for IS2 is obtained as

$$\begin{aligned} \eta_{IS}^i(k) &= \gamma_{IS}^i(k)^T \left[P_{IS}^i(k|k)\right]^{-1} \gamma_{IS}^i(k) \\ &= \left[\hat{x}_{m2}(k|k) - \hat{x}_i(k|k)\right]^T \left[P_i(k|k) - P_{m2}(k|k)\right]^{-1} \\ &\quad \cdot \left[\hat{x}_{m2}(k|k) - \hat{x}_i(k|k)\right]. \end{aligned} \tag{19}$$

Note that additional consideration is needed when the slip and slide errors are detected by the SSD algorithms considered in Section IV, where the estimate of the velocity local filter of the tachometer becomes $\hat{x}_1(k) = \hat{x}_{m1}(k)$, when the slip and slide error is detected. And when $\hat{x}_1(k) = \hat{x}_{m1}(k)$, it happens that η_{IS}^1 for IS2 becomes almost zero, which generates a singularity problem in calculating β_i using (14). To resolve such a problem, η_{IS}^1, that is related to the velocity local filter of the tachometer, is calculated as follows when the slip and slide errors are detected:

$$\eta_{IS}^1(k) = \frac{1}{M-1} \sum_{i=2}^{M} \eta_{IS}^i(k). \tag{20}$$

IV. Slip and Slide Detection Algorithm

Tachometer is a sensor to measure the rotational speed of a wheel to estimate the velocity of the train. However, the estimate accuracy of the tachometer degrades with the slip and slide of the wheel. It is necessary to check if the velocity estimate from the tachometer is within the normal range in order to detect the slip and slide errors. In general, the slip and slide errors tend to occur when the train is accelerating, decelerating or moving along a curved track [11]. In HST, it has been found that the slip and slide errors can cause a position error of from tens of meters to hundreds of meters.

A. Slip and Slide Detection

To detect the (wheel) slip and slide errors, one of the common techniques used in practice is to use a reference to compare with the tachometer measurements. In this paper, we propose two slip and slide detection (SSD) algorithms that utilize the position and velocity estimates from the TS-FKF for a reference. In the following, we introduce the two SSD algorithms in detail.

1) Proposed Slip and Slide Detection Algorithm Based on Position Estimate (SSD1): The first proposed SSD algorithm considered in this paper, denoted as SSD1 algorithm, uses the position estimate of the first master filter in the TS-FKF. Let γ^P_{SSD} be defined as the difference of the position estimates between the first master filter and the velocity local filter (the 1st local filter) for the tachometer, the superscript $(\cdot)^P$ represents the position, then

$$\gamma^P_{SSD}(k) = \hat{x}^P_{m1}(k|k) - \hat{x}^P_1(k|k) \tag{21a}$$

$$\begin{aligned} P^P_{SSD}(k) &= E\left[\gamma^P_{SSD}(k)\gamma^{P\ T}_{SSD}(k)\right] \\ &= P^P_{m1}(k|k) + P^P_1(k|k), \end{aligned} \tag{21b}$$

where $\hat{x}^P_{m1}$ and P^P_{m1} are the position estimate and its error covariance of the first master filter, respectively, $\hat{x}^P_1$ and P^P_1 represent the position estimate and its error covariance of the velocity local filter with the tachometer, respectively, and P^P_{SSD} is the covariance of γ^P_{SSD}.

Notice that the expression in (21b) is obtained with an assumption that $\hat{x}^P_{m1}$ and $\hat{x}^P_1$ are uncorrelated. In the proposed navigation system shown in Fig. 1, the estimate errors of all local filters are corrupted by the same process noise from INS and, therefore, are correlated [12]. However, when the federated filter operates in a feedback mode with appropriate information sharing, it is found that the cross-correlation between the local filters can be eliminated [12], and that the covariance P^P_{SSD} can be found as (21b). The test statistic η^P_{SSD} for the slip and slide detection with SSD1 algorithm is obtained as

$$\begin{aligned} \eta^P_{SSD}(k) &= \gamma^{P\ T}_{SSD}(k) P^{P-1}_{SSD}(k) \gamma^P_{SSD}(k) \\ &= \left[\hat{x}^P_{m1}(k|k) - \hat{x}^P_1(k|k)\right]^T \\ &\quad \times \left[P^P_{m1}(k|k) + P^P_1(k|k)\right]^{-1} \\ &\quad \times \left[\hat{x}^P_{m1}(k|k) - \hat{x}^P_1(k|k)\right], \end{aligned} \tag{22}$$

which has a chi-square distribution with 3 degrees of freedom. In SSD1, η^P_{SSD} is compared to a threshold T^P_{SSD} to detect the slip and slide as follows:

$$\begin{cases} \eta^P_{SSD}(k) > T^P_{SSD} & \text{Slip \& Slide detection} \\ \eta^P_{SSD}(k) \le T^P_{SSD} & \text{No Slip \& Slide,} \end{cases} \tag{23}$$

where T^P_{SSD} is determined from the chi-square distribution table.

2) Proposed Slip and Slide Detection Algorithm Based on Velocity Estimate (SSD2): The second proposed SSD algorithm, denoted as SSD2 algorithm, uses the velocity estimate of the first master filter in the TS-FKF. Let γ^V_{SSD} represent the difference of velocity estimates between the first master filter and the velocity local filter for the tachometer, where the superscript $(\cdot)^V$ represents the velocity. Using the same notations used in Section IV-A1, we can find the estimate and its covariance of the SSD2 algorithm as

$$\gamma^V_{SSD}(k) = \hat{x}^V_{m1}(k|k) - \hat{x}^V_1(k|k) \tag{24a}$$

$$\begin{aligned} P^V_{SSD}(k) &= E\left[\gamma^V_{SSD}(k)\gamma^{VT}_{SSD}(k)\right] \\ &= P^V_{m1}(k|k) + P^V_1(k|k), \end{aligned} \tag{24b}$$

respectively. The test statistic η^V_{SSD} for the SSD2 is derived as

$$\begin{aligned} \eta^V_{SSD}(k) &= \gamma^{V\ T}_{SSD}(k) P^{V\ -1}_{SSD}(k) \gamma^V_{SSD}(k) \\ &= \left[\hat{x}^V_{m1}(k|k) - \hat{x}^V_1(k|k)\right]^T \\ &\quad \times \left[P^V_{m1}(k|k) + P^V_1(k|k)\right]^{-1} \\ &\quad \times \left[\hat{x}^V_{m1}(k|k) - \hat{x}^V_1(k|k)\right], \end{aligned} \tag{25}$$

which has a chi-square distribution with 3 degrees of freedom and is used for the slip and slide detection as

$$\begin{cases} \eta^V_{SSD}(k) > T^V_{SSD} & \text{Slip \& Slide detection} \\ \eta^V_{SSD}(k) \le T^V_{SSD} & \text{No Slip \& Slide,} \end{cases} \tag{26}$$

where T^V_{SSD} is a threshold for SSD2 algorithm and is determined from the chi-square distribution table.

In general, the slip and slide errors cause the difference in the count of wheel rotation from a nominal wheel, and the velocity estimate generated from the tachometer is directly corrupted by the slip and slide errors. Therefore, the velocity estimate is directly influenced by the presence of the slip and slide errors, and it is expected that the SSD2 algorithm using the velocity estimate can have the better performance than the SSD1 algorithm using the position estimate.

B. Slip and Slide Compensation

When a slip or slide error occurs, the performance of the velocity local filter of the tachometer is deteriorated due to the measurement corrupted by the error, and the degraded estimates of velocity local filter of the tachometer are sent to the second master filter, causing a large navigation error. In addition, the navigation error of the TS-FKF is passed to the local filters so that the performance of local filters degrades dramatically.

To resolve such a problem, we employ a simple compensation scheme that when a slip or slide error is detected by the SSD algorithm, the estimate of the first master filter replaces that of the velocity local filter for the tachometer as

$$\hat{x}_1(k) = \hat{x}_{m1}(k). \tag{27}$$

The SSD algorithm and the compensation scheme in (27) are not computationally expensive so that they are suitable to the HST navigation system.

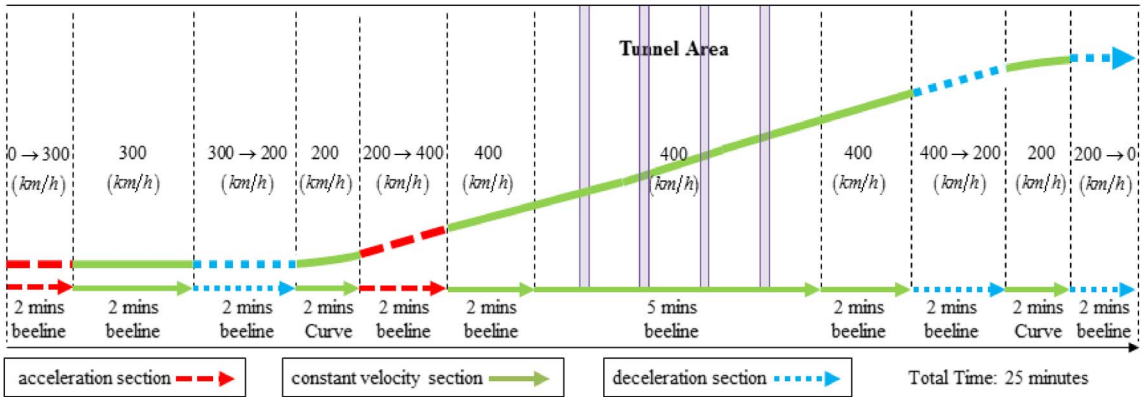

Fig. 2. Train trajectory.

TABLE II
SENSOR SPECIFICATION

	Update rate	White Noise(σ)	Random Bias	Deployment Spacing
Accelerometer	100 Hz	50 μg	1000 μg	·
Gyroscope	100 Hz	0.1 deg/h	1 deg/h	·
DGPS(position)	1 Hz	2 m	·	·
DGPS(velocity)	1 Hz	1 m/s	·	·
Tachometer	20 Hz	0.1 m/s	·	·
RFID	random	1 m	·	300 m

V. SIMULATION AND PERFORMANCE ANALYSIS

In this section, the proposed HST navigation system based on the TS-FKF is simulated with MATLAB and the performance is analyzed. In addition, we test the two IS algorithms and the two SSD algorithms considered in previous sections with separate simulations and show that the proposed algorithms are performing most reliably in the propose system as expected.

A. Simulation Conditions

1) Simulated Train Trajectory: In the simulations to test the proposed system, we design the railway trajectory considering the characteristics of the express railways in Korea. It consists of sections of straight tracks and curved tracks where trains are accelerating, decelerating and moving with a constant velocity as shown in Fig. 2. The maximum speed is set to 400 km/h and the total travel distance is 120 km with overall travel time of 25 minutes. There exist four tunnels inside 400 km/h constant velocity section, and each tunnel is 555 m long.

2) Sensor Specification: The characteristics of inertial sensors, such as accelerometers and gyroscopes, and other sensors used in the simulations are summarized in Table II. All inertial sensors are operating at an update rate of 100 Hz. The update rates of the other sensors and RFID deployment spacing are also summarized in Table II. The DGPS is operating at 1 Hz, but the tachometer updates at 20 Hz. The update rate of RFID depends on the RFID tag deployment spacing and the train speed. Thus, we assume it is random. In the simulations, RFID tags are deployed along railway tracks and their spacing is 300 m.

3) Slip and Slide Errors: Fig. 3 shows the velocity information obtained from the tachometer simulated with and without slip and slide errors. The slip and slide errors are inserted four times at four different locations along the track as Fig. 3; there are two (1st and 2nd) slip intervals and two (1st and 2nd) slide intervals occurring at separate locations. It is assumed that the duration of the slip or slide error is 20 seconds when it occurs. Note that as shown in Fig. 3, a slip and slide error causes a higher and lower speed reading from the tachometer than the actual speed, respectively.

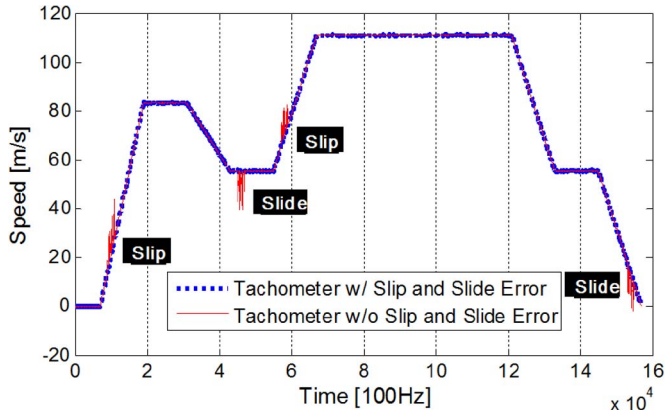

Fig. 3. Slip and slide error.

B. Performance Analysis

1) Performance Analysis for IS Algorithms: In this subsection, the performance of the proposed system is tested with simulations, and the proposed IS algorithms and SSD algorithms are applied in the simulations. The performance is compared with simulations with and without the slip and slide errors.

The left side of Fig. 4 shows position RMS (Root Mean Square) errors of the second master filter for the two IS algorithms (IS1 and IS2) in the absence of slip and slide errors. As shown, IS2 shows a smaller RMS error than IS1. The right side of Fig. 4 shows position RMS errors for the two IS algorithms in the presence of slip and slide errors. The total RMS errors of the right side are much larger than those of the left side due to the slip and slide errors. In the presence of the slip and slide errors, each local filter has a different performance, and, therefore, the proposed adaptive IS2 algorithm shows a better

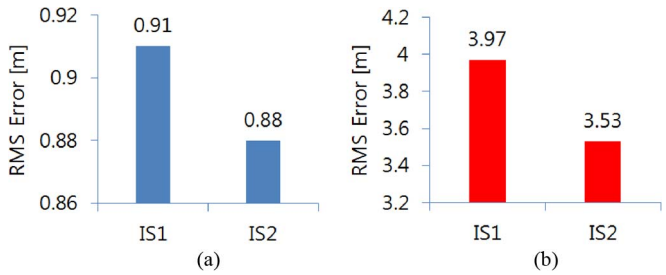

Fig. 4. Second master filter results of position RMS errors of two IS algorithms. (a) Without slip&slide error. (b) With slip&slide error.

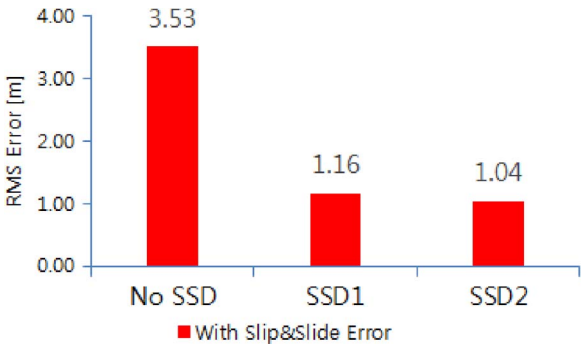

Fig. 5. 2nd master filter result of position RMS errors of two SSD algorithms.

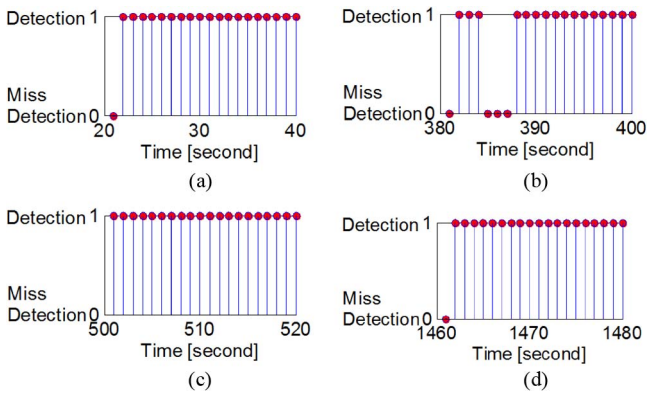

Fig. 6. Detection performance of SSD1. (a) 1st slip detection. (b) 1st slide detection. (c) 2nd slip detection. (d) 2nd slide detection.

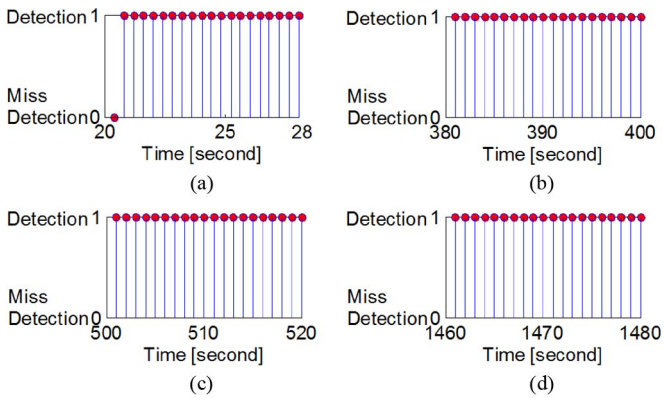

Fig. 7. Detection performance of SSD2. (a) 1st slip detection. (b) 1st slide detection. (c) 2nd slip detection. (d) 2nd slide detection.

performance comparing to the IS1 algorithm. As shown, the IS2 algorithm shows a much smaller position RMS error than the conventional IS1 algorithm. As a result, we conclude that the proposed IS2 algorithm has a better performance than the conventional IS algorithm (IS1).

2) Performance Analysis for SSD Algorithms: In this subsection, the performance of the proposed system is analyzed with simulations for the two SSD algorithms. In the simulations, we employ the proposed IS2 algorithm as shown in Section V-B1.

a) Comparison of position RMS errors: Fig. 5 shows position RMS errors of the second master filter for the two SSD algorithms in the presence of the slip and slide errors. For the proposed navigation system without an SSD algorithm, the position RMS error is 3.53 m, whereas others with an SSD algorithm show a much smaller RMS error. As shown in Fig. 5, the SSD2 algorithm based on velocity estimate shows the smallest RMS error and SSD1 based on position estimate shows the second smallest RMS error.

b) Performance comparison of the slip and slide error detection: To evaluate the performance of an SSD algorithm, it is essential to see the detection performance of the algorithm. For an SSD algorithm, the detection performance is strongly related to the determination of the detection threshold. In case of the proposed SSD algorithms, i.e., SSD1 and SSD2, thresholds are determined from the chi-square distribution table for a target false alarm probability. In the simulations, the false alarm probability for the SSD1 and SSD2 algorithms is set to 0.01.

The detection performance of the SSD1 and SSD2 algorithms is compared in more detail as in Figs. 6 and 7, respectively. The two figures on the left of Figs. 6 and 7 show the slip detection performance at the 1st and 2nd slip intervals, and the two figures on the right show the slide detection performance at the 1st and 2nd slide intervals. In the figures, a successful detection and a detection failure are represented by a bar with unit amplitude and a bar with zero amplitude, respectively. As shown, Fig. 6 shows the SSD1 algorithm misses the detection of the slip for one instant during the 1st slip interval and none during the 2nd slip interval. In the 1st slide interval and the 2nd slide interval detection, there are four and one miss-detections, respectively. The detection performance of the SSD2 algorithm is shown in Fig. 7, where only one miss-detection of the slip occurs. Therefore, from the simulation results, the SSD2 algorithm shows a better detection performance.

c) Contribution of SSD2 algorithm to the proposed system: In this subsection, we compare the horizontal position errors of the proposed system with and without the SSD2 algorithm. The train is on the East bound, and IS2 algorithm is employed in the simulations. Fig. 8 shows the East-West components of the position errors on the left and the North-South components on the right during the whole simulation interval. In left figure, it shows that the large East-West position error exists four times due to the two slip and two slide intervals. From Fig. 8, we can see that the large slip and slide errors are removed by the SSD2 algorithm appropriately.

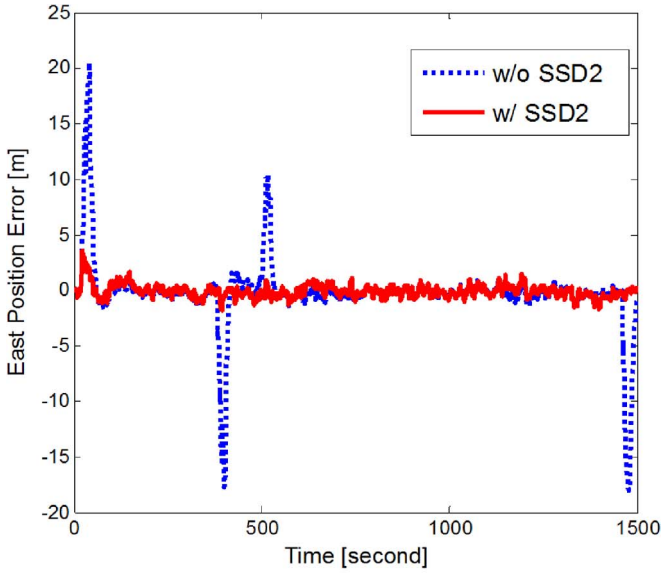

(a)

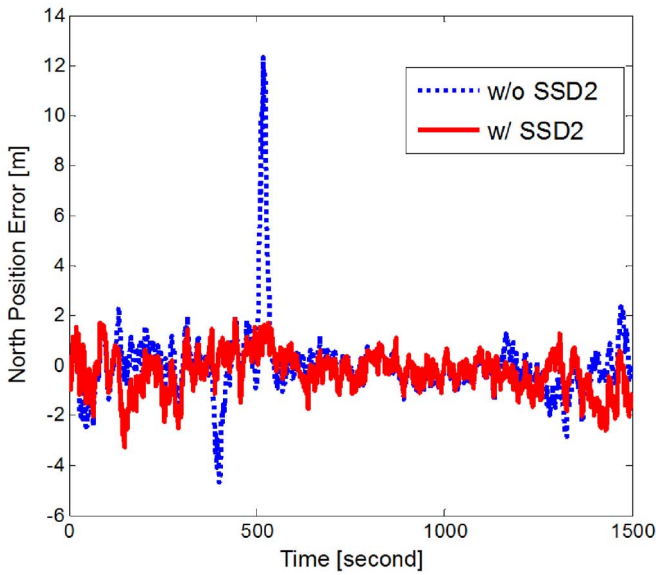

(b)

Fig. 8. Contribution of the SSD2 algorithm to the proposed system. (a) East. (b) North.

Note that the conventional KF based HST navigation algorithms [1], [2], [4] can have the similar performance to the simulation results without the SSD algorithm shown in Fig. 8. From simulation results, we conclude that the proposed system based on TS-FKF with the IS2 and SSD2 algorithms show a strong performance improvement and robustness to the slip and slide errors.

VI. Conclusion

In this paper, a TS-FKF based navigation system has been proposed for high-speed trains, where the TS-FKF is designed to process measurements from multi-sensors such as the tachometer, inertial sensors, DGPS, and RFID. In addition, a detection algorithm and an adaptive information sharing algorithm have been proposed to detect the slip and slide errors in the tachometer measurements and to deal with problems such as large tachometer error and the performance difference between sensors, respectively. Theoretical analysis and simulation results have demonstrated that the performance of the proposed system is improved with the proposed algorithms. In addition, it has been found that the proposed adaptive information sharing algorithm has a simple structure to implement and low computational complexity. Therefore, the proposed system with the proposed algorithms is suitable to the navigation system for high-speed trains.

Appendix A

The matrix H_s (5a) is defined as follows.

$$H_s = -2\begin{bmatrix} C_{13}V_E - C_{12}V_D & C_{11}V_D - C_{13}V_N \\ C_{23}V_E - C_{22}V_D & C_{21}V_D - C_{23}V_N \\ C_{33}V_E - C_{32}V_D & C_{31}V_D - C_{33}V_N \end{bmatrix} \begin{bmatrix} C_{12}V_N - C_{11}V_E \\ C_{22}V_N - C_{21}V_E \\ C_{32}V_N - C_{31}V_E \end{bmatrix} \times \begin{bmatrix} -q_1 & q_0 & -q_3 & q_2 \\ -q_2 & q_3 & q_0 & q_1 \\ -q_3 & -q_2 & q_1 & q_0 \end{bmatrix}$$

where

$$C_n^b = \begin{bmatrix} C_{11} & C_{12} & C_{13} \\ C_{21} & C_{22} & C_{23} \\ C_{31} & C_{32} & C_{33} \end{bmatrix},$$

$$Q_n^b = \begin{bmatrix} q_0 & q_1 & q_2 & q_3 \end{bmatrix}.$$

Appendix B

The following defines errors as

$$e_{m2}(k|k) = x(k) - \hat{x}_{m2}(k|k) \quad \text{(B-.1)}$$

$$e_i(k|k) = x(k) - \hat{x}_i(k|k). \quad \text{(B-.2)}$$

Here, we assume that all local filters and the second master filter are unbiased estimators and the expectations of the errors in (B-.1) and (B-.2) are zeros such that

$$E\left[e_{m2}(k|k)\right] = 0, \quad E\left[e_i(k|k)\right] = 0. \quad \text{(B-.3)}$$

Lemma B.-1: The error cross-covariance $P_{i,m2}(k|k)$ and $P_{m2,i}(k|k)$ are defined as

$$P_{i,m2}(k|k) = E\left[e_i(k|k)e_{m2}^T(k|k)\right] \quad \text{(B-.4)}$$

$$P_{m2,i}(k|k) = E\left[e_{m2}(k|k)e_i^T(k|k)\right]. \quad \text{(B-.5)}$$

For $E[\gamma_{IS}^i(k)] = 0$ as in (B-.3), the covariance P_{IS}^i is found as

$$P_{IS}^i(k) = P_i(k|k) - P_{i,m2}(k|k) - P_{m2,i}(k|k) + P_{m2}(k|k). \quad \text{(B-.6)}$$

Proof: In case that $E[\gamma_{IS}^{i}(k)] = 0$, P_{IS}^{i} is defined as

$$P_{IS}^{i}(k) = E\left[\gamma_{IS}^{i}(k){\gamma_{IS}^{i}}^{T}(k)\right]. \tag{B-.7}$$

Using (B-.3), (B-.7) is derived as

$$\begin{aligned}
P_{IS}^{i}(k) &= E\left[\gamma_{IS}^{i}(k)\gamma_{IS}^{iT}(k)\right] \\
&= E\left[\left[e_i(k|k) - e_{m2}(k|k)\right]\left[e_i(k|k) - e_{m2}(k|k)\right]^T\right] \\
&= E\left[e_i(k|k)e_i^T(k|k) - e_i(k|k)e_{m2}^T(k|k)\right. \\
&\qquad \left. - e_{m2}(k|k)e_i^T(k|k) + e_{m2}(k|k)e_{m2}^T(k|k)\right] \\
&= E\left[e_i(k|k)e_i^T(k|k)\right] - E\left[e_i(k|k)e_{m2}^T(k|k)\right] \\
&\quad - E\left[e_{m2}(k|k)e_i^T(k|k)\right] \\
&\quad + E\left[e_{m2}(k|k)e_{m2}^T(k|k)\right] \\
&= P_i(k|k) - P_{i,m2}(k|k) - P_{m2,i}(k|k) \\
&\quad + P_{m2}(k|k).
\end{aligned} \tag{B-.8}$$

■

Lemma B-.2: From (B-.3), it is proved that $P_{m2,i}(k|k) = P_{m2}(k|k)$.

Proof:

$$\begin{aligned}
P_{m2,i}(k|k) &= E\left[x(k)x^T(k)\right] - E\left[\hat{x}_{m2}(k|k)\hat{x}_i^T(k|k)\right] \\
&= E\left[x(k)x^T(k)\right] \\
&\quad - E\left[P_{m2}(k|k) \times \left[\sum_{j=1}^{M} P_j^{-1}(k|k)\hat{x}_j(k|k)\right]\right. \\
&\qquad \left. \times \hat{x}_i^T(k|k)\right] \qquad \text{(B-.9)} \\
&= E\left[x(k)x^T(k)\right] \\
&\quad - E\left[P_{m2}(k|k)\sum_{j=1}^{M} P_j^{-1}(k|k)\hat{x}_j(k|k)\hat{x}_i^T(k|k)\right] \\
&= E\left[x(k)x^T(k)\right] - P_{m2}(k|k) \\
&\quad \times \begin{bmatrix} P_1^{-1}(k|k)E\left[\hat{x}_1(k|k)\hat{x}_i^T(k|k)\right] + \cdots \\ + P_i^{-1}(k|k)E\left[\hat{x}_i(k|k)\hat{x}_i^T(k|k)\right] + \cdots \\ + P_M^{-1}(k|k)E\left[\hat{x}_M(k|k)\hat{x}_i^T(k|k)\right] \end{bmatrix} \\
&= P_{m2}(k|k)\left[\sum_{j=1}^{M} P_j^{-1}(k|k)\right] E\left[x(k)x^T(k)\right] \\
&\quad - P_{m2}(k|k) \\
&\quad \times \begin{bmatrix} P_1^{-1}(k|k)E\left[\hat{x}_1(k|k)\hat{x}_i^T(k|k)\right] + \cdots \\ + P_i^{-1}(k|k)E\left[\hat{x}_i(k|k)\hat{x}_i^T(k|k)\right] + \cdots \\ + P_M^{-1}(k|k)E\left[\hat{x}_M(k|k)\hat{x}_i^T(k|k)\right] \end{bmatrix}
\end{aligned} \tag{B-.10}$$

$$\begin{aligned}
&= P_{m2}(k|k)P_1^{-1}(k|k) \\
&\quad \times \left\{E\left[x(k)x^T(k)\right] - E\left[\hat{x}_1(k|k)\hat{x}_i^T(k|k)\right]\right\} \\
&\quad + \cdots + P_{m2}(k|k)P_i^{-1}(k|k) \\
&\quad \times \left\{E\left[x(k)x^T(k)\right] - E\left[\hat{x}_i(k|k)\hat{x}_i^T(k|k)\right]\right\} \\
&\quad + \cdots + P_{m2}(k|k)P_M^{-1}(k|k) \\
&\quad \times \left\{E\left[x(k)x^T(k)\right] - E\left[\hat{x}_M(k|k)\hat{x}_i^T(k|k)\right]\right\} \\
&= P_{m2}(k|k)\left[P_1^{-1}(k|k)P_{1i}(k|k) + \cdots \right. \\
&\qquad \left. + P_i^{-1}(k|k)P_i(k|k) + \cdots \right. \\
&\qquad \left. + P_M^{-1}(k|k)P_{Mi}(k|k)\right] \\
&= P_{m2}(k|k)\left[P_i^{-1}(k|k)P_i(k|k)\right] \\
&= P_{m2}(k|k),
\end{aligned} \tag{B-.11}$$

where the expressions (B-.9) and (B-.10) are derived from (10) and (9), respectively. ■

REFERENCES

[1] A. Genghi *et al.*, "The RUNE project: Design and demonstration of a GPS/EGNOS-based railway user navigation equipment," in *Proc. ION GNSS*, Portland, OR, USA, Sep. 2003, pp. 225–237.

[2] H. Zhang, J. Rong, and X. Zhong, "Research of the INS/GPS integrated navigation system for high speed trains," in *Proc. IEEE 9th ICYCS*, Hunan, China, Nov. 2008, pp. 1659–1663.

[3] K. Kim, S. Seol, and S.-H. Kong "High accuracy navigation system based on multisensor data fusion and map matching algorithm," *Int. J. Control Autom. Syst.*, vol. 13, no. 3, pp. 1–10, Jun. 2015.

[4] R. Mázl and L. Přeučil, "Sensor data fusion for inertial navigation of trains in GPS-dark areas," in *Proc. IEEE Int. Veh. Symp.*, Columbus, OH, USA, Jun. 2003, vol. 1, pp. 345–350.

[5] S.-H. Kong and W. Nam, "A-GNSS sensitivity for parallel acquisition in asynchronous cellular networks," in *IEEE Trans. Wireless Commun.*, vol. 9, no. 12, pp. 3770–3778, Dec. 2010.

[6] B. G. Cai, J. Wang, Q. Yin, and J. Liu, "A GNSS based slide and slip detection method for train positioning," in *Proc. ACIP*, Jul. 2009, vol. 1, pp. 450–453.

[7] C. C. Ward and K. Iagnemma, "A dynamic-model-based wheel slip detector for mobile robots on outdoor terrain," *IEEE Trans. Robot.*, vol. 24, no. 4, pp. 821–831, Aug. 2008.

[8] K. Iagnemma and C. C. Ward, "Classification-based wheel slip detection and detector fusion for mobile robots on outdoor terrain," *Auton. Robots*, vol. 26, no. 1, pp. 33–46, Jan. 2009.

[9] D. Sellers, "Development of a slip detection technique for the AIRTRANS rubber-tired vehicle," in *Conf. Rec. 15th IEEE IAS Annu. Meeting*, Cincinnati, OH, USA, Sep./Oct. 1980, pp. 214–220.

[10] E. J. Lee *et al.*, "Slip/slide detection method for the railway vehicles using rotary type speed sensor," in *Proc. KIEE Conf.*, Muju, Korea, 2000, pp. 405–407.

[11] S. S. Saab, G. E. Nasr, and E. A. Badr, "Compensation of axle-generator errors due to wheel slip and slide," *IEEE Trans. Veh. Technol.*, vol. 51, no. 3, pp. 577–587, May 2002.

[12] N. A. Carlson, "Federated square root filter for decentralized parallel processes," *IEEE Trans. Aerosp. Electron. Syst.*, vol. 26, no. 3, pp. 517–525, May 1990.

[13] N. A. Carlson and M. P. Berarducci, "Federated Kalman filter simulation result," *Navigation*, vol. 41, no. 3, pp. 297–322, Fall 1994.

[14] R. H. Liu and J. Y. Liu, "A new method of information sharing in federated filter," *J. Chin. Inertia. Technol.*, vol. 9, no. 2, pp. 28–32, Feb. 2001.

[15] W. Qiuping, G. Zhongyu, and W. Dejun, "An adaptive information fusion method to vehicle integrated navigation," in *Proc. IEEE PLANS*, Palm Springs, CA, USA, Apr. 2002, pp. 248–253.

[16] H. Zhang, B. Lennox, P. R. Goulding, and Y. Wang, "Adaptive information sharing factors in federated Kalman filtering," in *Proc. 15th IFAC World Congr.*, Barcelona, Spain, 2002, pp. 664–664.

[17] Z. Xiong, J. Chen, R. Wang, and J. Liu, "A new dynamic vector formed information sharing algorithm in federated filter," *Aerosp. Sci. Technol.*, vol. 29, no. 1, pp. 37–46, Aug. 2013.

[18] D. H. Titterton and J. L. Weston, *Strapdown Inertial Navigation Technology*, 2nd ed. London, U.K.: IET, 2004.

Kwanghoon Kim received the Ph.D. degree in electrical engineering and computer science from Seoul National University, Seoul, Korea, in 2006. He is currently a Research Professor at the CCS Graduate School for Green Transportation, Korea Advanced Institute of Science and Technology, Daejeon, Korea. His research interests include fault detection, Kalman filtering, GNSS/INS integration system, and GNSS signal processing algorithms.

Seung-Hyun Kong (M'06) received the B.S. degree in electronics engineering from Sogang University, Seoul, Korea, in 1992, the M.S. degree in electrical engineering from New York University Polytechnic School of Engineering, Brooklyn, NY, USA, in 1994, and the Ph.D. degree in aeronautics and astronautics from Stanford University, Stanford, CA, USA, in 2006. From 1997 to 2004, he was with Samsung Electronics Inc. and Nexpilot Inc., both in Korea, where his research focus was on wireless communication systems and UMTS mobile positioning technologies. In 2006 and from 2007 to 2009, he was a Staff Engineer at Polaris Wireless Inc., Santa Clara, CA, and at the Corporate R&D, Qualcomm Inc., San Diego, CA, respectively, where his research was on assisted GNSS and wireless positioning technologies such as wireless location signature and mobile-to-mobile positioning technologies. Since 2010, he has been with the Korea Advanced Institute of Science and Technology, where he is currently an Associate Professor at the CCS Graduate School for Green Transportation. His research interests include next-generation GNSS, advanced signal processing for navigation systems, and vehicular communication systems.

Sang-Yun Jeon received the B.S. degree from the Korea Advanced Institute of Science and Technology, Daejeon, Korea, in 2014, where he is currently working toward the M.S. degree at the CCS Graduate School for Green Transportation. His research interests include sensor fusion, detection and estimation in navigation systems, and positioning technologies.